Journal of Chemistry Studies
DOI: 10.32996/jcs
Journal Homepage: www.al-kindipublisher.com/index.php/jcs

JCS
AL-KINDI CENTER FOR RESEARCH AND DEVELOPMENT

| RESEARCH ARTICLE

ZnO Nanorods Growth and the Parametric Survey of Factors Influencing the Morphologies for DSSC Application-Review

Salisu I. Kunya[1] ✉ Yunusa Abdu[2], Mohd Kamarulzaki Mustafa[3] and Mohd Khairul Ahmad[4]

[1]Department of Science laboratory Technology, Jigawa State Polytechnics, Dutse, Nigeria; Department of Physics, Faculty of Physical Sciences, College of Natural and Pharmaceutical Sciences, Bayero University, Kano, Nigeria; Department of Physics and Chemistry, Faculty of Applied Sciences and Technology, Universiti Tun Hussein Onn Malaysia (UTHM), Kampus Pagoh, Jalan Panchor 84000 Muar, Johor, Malaysia

[2]Department of Physics, Faculty of Physical Sciences, College of Natural and Pharmaceutical Sciences, Bayero University, Kano, Nigeria

[3]Department of Physics and Chemistry, Faculty of Applied Sciences and Technology, Universiti Tun Hussein Onn Malaysia (UTHM), Kampus Pagoh, Jalan Panchor 84000 Muar, Johor, Malaysia

[4]Microelectronic and Nanotechnology–Shamsuddin Research Centre (MiNT-SRC), Faculty of Electrical and Electronic Engineering, Universiti Tun Hussein Onn Malaysia (UTHM), Parit Raja, Batu Pahat Johor, 86400, Malaysia

Corresponding Author: Salisu I. Kunya, **E-mail**: salisukunya2016@gmail.com

| ABSTRACT

Zinc-oxide (ZnO) nanostructures, such as nanorods, are generally viewed as leading studies of keen interest due to their significant application potential in many applied areas, primarily for the improvement of photovoltaic solar cells. The morphologies of nanorods are linked to the seed layer (SL) optimization. As a result, forming a high-quality ZnO thin film prior to the growth of nanorods is critical. The processing parameters used during the synthesis technique can influence the quality of the synthesized samples. This review article focuses on the outcomes of the process variables responsible for better-synthesized ZnO SL for nanorod growth. The effect of various parameters, such as annealing temperature, precursor solution, and ZnO SL thickness, on the morphology characteristics of ZnO nanorods prepared was reviewed. The study examined numerous published works to find the effect of heat treatment, the thickness of the layer, substrate, and precursor concentration on the morphology of the seed layer in the production of ZnO nanorods.

| KEYWORDS

Morphology, Zinc-oxide nanorods, Zinc-oxide seed layer

| ARTICLE INFORMATION

ACCEPTED: 31 August 2022 **PUBLISHED:** 31 September 2022 **DOI:** 10.32996/jcs.2022.1.2.3

1. Introduction

Energy is the backbone of mankind. Day after day, human energy consumption levels necessitate the usage of green energy. Accordance to Energy Information Administration, the global energy requirements are expected to grow by 28% between 2015 and 2040, from 19.2 to 24.6 TWy (Carella et al., 2018). Solar cell technology has been identified as a viable renewable energy source for meeting rising global energy demand with minimal environmental impact (Weerasinghe et al., 2013). The tenet of photosynthesis is used in DSSCs. It is a single-junction solar cell from the third-generation family (Bera et al., 2021). This generation of solar cells is expected to surpass the Shockley– Queisser limit of 31–41% power efficiency (Shakeel Ahmad et al., 2017). The Shockley–Queisser efficiency limit, or a detailed balance limit, is a theoretical estimation of the maximum limit for solar cell efficiency. This limit only applies to idealized p-n junction cells (Jacak & Jacak, 2022). DSSC produced charge carriers independent

of the p-n junction. Grátzel and O'Regan discovered the innovation in 1991. Grátzel and his Coworker used a ruthenium-based dye and 10-μm thick porous TiO2 nanoparticle films (Rho et al., 2015). The cell's power conversion efficiency (PCE) was 7%, which was high enough to grab attention in similar cells.

The main advantages of DSSCs are fully biodegradable, non-toxic, and cheaper than traditional p-n junction solar cells (Parisi et al., 2017). Many methods for increasing efficiency were mentioned, including promoting electron transfer via film electrodes and preventing or minimizing electron recombination between the substrate and another interface (Pavithra et al., 2015), optimizing annealing temperature, and incorporating a nanorod layer into the photoanode are all crucial steps in achieving repeatable device performance. It has been documented that ZnO films serve as the nucleation site for the formation of ZnO NRs. Controlling the morphology of ZnO films results in final ZnO NRs with well-defined positions and orientations (Mbuyisa et al., 2015). The diameter of the ZnO nanorods grown appears to be determined by the seed layer's properties rather than the initial growth time and temperature. The length of the nanorods, on the other hand, is governed by the growth time, temperature, and Zn2+ concentration in the solution (Yin et al., 2010).

Much work has gone into studying the effect of reaction conditions on ZnO nanowires. Many researchers concentrated on the seeding layer effect, chemical reagents, and the concentration effect on ZnO nanowire density, morphology, growth time, and temperature. Thus, the goal is to review the impact of the above parameters on ZnO nanostructure morphology under various fabrication scenarios. ZnO nanostructures can be in solution or gaseous form. Water is used in solution phase synthesis because of its simplicity and reasonable growth conditions. The hydrothermal approach to generating ZnO nanostructures has gained enormous appeal. Because the synthesis takes place in an aqueous solution, the growth temperatures are lower than the boiling point of water.

2. Photoanode

The metal oxide semiconductor is among the components of a photoanode. The semiconductors served as electron carriers and dye adsorption surfaces (Pallikkara & Ramakrishnan, 2020). Examples of metal oxide are; TiO_2, ZnO, SnO_2, and Nb_2O_5. The energy levels of the valence band and conduction band are considered to choose the said metal oxide for effective charge separation and reduced recombination**.**

2.1 Zinc oxide (ZnO)

ZnO is an n-type semiconductor having a wide band-gap of $3.3eV$ (Fang et al., 2020) and higher electron mobility of about $60meV$ (Siregar et al., 2020). The Wurtzite-type structure is formed by ZnO in its thermodynamically stable state. Wurtzite-type ZnO is polar because the oxygen and zinc atoms are interlaced along the c-axis (Nowak et al., 2020). ZnO is also recognized as a polymorph, with diverse types of a structure subject to the synthesis method. ZnO nano morphology includes nanospheres, nanowires, nanorods, nanoflower, nanotubes, nanocrystals, and 3D nanostructures (core-shell) (Wibowo et al., 2020). As pure ZnO thin films are delicate to oxidation, absorption of O_2 in the films is inclined to decrease the electrical conductivity (Lee & Park, 2003). When a ZnO seed layer is immersed in a highly concentrated Zn ion solution, the ZnO nanorod begins to grow along the strong priority plane due to following reasons: the plane has top surface energy and rising velocity, as well as the dense seed layer's intense initiation and space constraint.

2.2.1 Application of Zinc Oxide

1. ZnO is vibrant in optoelectronics and laser skill because of its wide-ranging energy band (3.37 eV), great bond energy (60 meV), and great thermal and mechanical firmness at low temperature
2. Because of high-voltage obstructive competency, great temperature process, and high changing frequencies, most of the extensive bandgap semiconductors could be practically useful in power electronics
3. It can be essential as a sensor, converter, energy initiator, and photocatalyst in hydrogen creation for its piezoelectric and pyroelectric properties
4. Zinc oxide material is being used in the ceramics industry owing to its hardness, rigidity, and piezoelectric constant
5. It is a central material for biomedicine and pro-ecological systems applications due to its short toxicity plus biodegradability.

3. Hydrothermal Technique

The term hydrothermal derives entirely from geology. Sir Roderick Murchison (1792–1871) coined the term to describe the action of water at high temperatures and pressures in causing changes in the earth's crust, resulting in the formation of various rocks and minerals (Yoshimura & Byrappa, 2008). These days, hydrothermal technology is in use in the synthesis of single-crystal such as ZnO, and GaN, among others.

The hydrothermal and solvothermal techniques are quite similar, with the precursor solutions being the key difference.

In the hydrothermal and solvothermal techniques, respectively, aqueous and non-aqueous precursor solutions are employed. The principal chemical processes take place in a stainless steel Teflon autoclave at high temperatures and pressures. The dielectric constant and viscosity of H_2O drop with increasing temperature and increase with expanding pressure in the hydrothermal process, with the temperature impact being the most. The increased temperature within a hydrothermal system has a significant effect on sample solubility and solids transport due to changes in such H_2O properties (Verma et al., 2017).

3.1 Advantages of Hydrothermal Method

1. It does not require the use of organic solvents or additional processing of the product (grinding and calcination), which makes it a simple and environmentally friendly technique.
2. The method resulted in diverse shapes and dimensions of the resulting crystals depending on the composition of the starting mixture and the process temperature and pressure,
3. Formation of a high degree of pure crystalline product,

4. Hydrothermal techniques for the growth of ZnO nanorods

The structure of ZnO NRs occurs primarily in two paths: the main is the development of ZnO nuclei, also known as nucleation, and the next is the growth of ZnO NRs. The basic framework for stage one is forming a precursor solution comprising zinc salt $Zn(NO_3)_2$, $ZnCl_2$, etc.) and an alkaline reagent such as; NaOH, hexamethylenetetramine (HMTA), Na_2CO_3, ammonia, and ethylenediamine. Organic surfactants, such as polyethyleneimine (PEI), have recently been used to further orient the nucleation of ZnO due to their ability to preferentially adsorb onto the lateral non-polar surfaces of growing NRs (Resmini et al., 2015).

The hydrothermal method for growing ZnO nanorods (NRs) is as follows, the nutrient solution of the required concentration will be prepared by combining an appropriate amount of alkaline reagent and Zinc salt nitrate in a given volume of solvent (e.g., deionized water). The mixture is stirred for at least 15 minutes until it dissolves. Then, the glass substrate made of a seed layer will be immersed in nutrient solution at $45^{0,}$ the layer facing the wall of the autoclave. Transfer the autoclave to the oven and heat for 3 hours or more at a low temperature. To regulate the flow of Hydroxyl ions, the temperature and pressure of the mixture in a Teflon-sealed stainless autoclave are necessary.

4.1 The Reaction Mechanism for Synthesis of ZnO using Hydrothermal Method

The hydrothermal mechanism comprises dissolution–precipitation or dissolution–crystallization. In the first stages of development, particles of the preparatory material dissolve in the solvent, forming ions or ionic clusters (Edalati et al., 2016). The solubility of the mixture increases as the temperature goes up; subsequently, the formation of yield product at super saturation state, as a result of the nucleation and particle growth state. These procedures are usually carried out in a closed environment. In the formation of the ZnO seed layer, the guiding equation is as follows

$$Zn(CH_3COO)_2.2H_2O \rightarrow Zn^{2+} + 2CH_3COO^- + 2H_2O \quad (1)$$

$$CH_3COO^- + H_2O \rightarrow CH_3COOH + OH^- \quad (2)$$

$$2OH^- + Zn^{2+} \rightarrow Zn(OH)_2 \quad (3)$$

$$Zn(OH)_2 \rightarrow ZnO + H_2O \quad (4)$$

Subsequently, during thermal annealing, the liquid evaporates, leaving only ZnO NPs on the glass substrates that act as the nucleation layer for the growth of ZnO NRs. Similarly, the reaction that explains the formation of ZnO NRs is presented below

$$Zn(NO_3)_2.6H_2O \rightarrow Zn^{2+} + 2NO_3^- + 6H_2O \quad (5)$$

$$(CH_2)_6N_4 + 6H_2O \rightarrow 6HCHO + 4NH_3 \quad (6)$$

$$NH_3 + H_2O \leftrightarrow NH_4^+ + OH^- \quad (7)$$

$$2OH^- + Zn^{2+} \rightarrow Zn(OH)_2 \quad (8)$$

$$Zn(OH)_2 \rightarrow ZnO + H_2O \quad (9)$$

Once zinc nitrate hexahydrate and HMTA are melted in DI water, they decompose into Zn^{2+} and OH^- ions, respectively. As soon as the ionic concentrations of these two ions reach supersaturation levels, they will conglomerate to form zinc hydroxide $Zn(OH)_2$. Because of the great temperature, $Zn(OH)_2$ dissolves into their individual ions, forming satisfactory ZnO NPs in the aqueous solution. These ZnO NPs will currently serve as nuclei for more growth, combining with the nucleation layer formed previously by the thermal decomposition of zinc acetate to diminish interfacial free energy.

5. Equivalent Circuit for the Dye Synthesize Solar Cell

The equivalent circuit is to understand the mechanism of DSSC and is presented in fig 1.

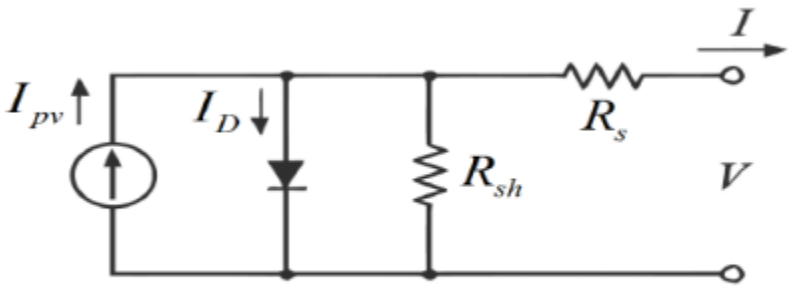

Figure 1. Equivalent circuit for DSSC

The relationship between external current and voltage is (Safriani et al., 2017)

$$I = I_{ph} - I_o \exp\left(\frac{-q(V-IR_s)}{nK_BT}\right) + \frac{V-IR_s}{R_{sh}} \quad (10)$$

Where, I_p is photogenerated current, I_o= dark saturation current, n is ideality factor, R_s is the series resistance R_{sh} is shunt resistance, K_B is Boltzmann's constant, q is a charge, and T is absolute temperature, n is the ideality factor it approaches to unity at high Fermi level

The power conversion efficiency is; (Savari et al., 2021)

$$\eta = \frac{V_{OC}J_{SC}FF}{P_{in}} \times 100 \quad (11)$$

Where V_{OC} is open circuit voltage, J_{sc} is short circuit current, FF is filled factor, and P_{in} is the power of the incident light.

6. Review of related literature

ZnO nanostructures can be developed in solution or gaseous form. Gas phase synthesis methods are complex and costly. Water is most often used in solution phase synthesis. Because of its straightforwardness and liveable growth conditions, the hydrothermal technique for producing ZnO nanostructures has garnered overwhelming support. Because the synthesis takes place in an aqueous solution, the growth temperatures are lower than the boiling point of water (Baruah & Dutta, 2009). Faisal et al. (2020) research the synthesis of ZnO nanorods on a silicon substrate. The existence of submicron and nanosized rods of varying lengths was confirmed by magnified SEM images. Nanorods are distributed across the substrate with a mean diameter of 75 nm and a length of 400 nm. Chalangar (et al., 2021) successfully grew vertically aligned ZnO nanorods with controllable diameter and density Using Sol-gel Seeding and Colloidal Lithography Patterning. Findings show that two-step dip-coating enhances the smoothness and crystal grain size of the seed layer, leading to a superior NR alignment. Kumar et al. (2021) studied the effects of reaction time on surface morphology, crystallinity, and bandgap energy in the synthesis of ZnO NRs. The maximum photovoltaic efficiency was 1.62 percent; however, by introducing a TiO_2 layer on the surface of the ZnO NRs in the photoanodes, the output of the DSSCs doubled. Boukhoubza et al. (2021) used the hydrothermal method to create ZnO nanorods with altered compositions of reduced graphene oxide. The existence of rod-like nanostructures characterizes the morphology of as-prepared samples. The typical particle dimension of samples determined by microstructural and morphological evaluations is closely related.

Kouhestanian et al. (2021) investigated the effect of width on the performance of the ZnO photo-anode of ZnO/N719-based DSSC. The finding shows that a photo-anode of thickness 19 µm produces 3.22%. Bourfaa et al. (2020) investigate the effect of seed layer surface position on the morphology of ZnO nanorods. The Micrographs revealed dense nanostructured structures on a glass substrate. ZnO nanorods are hexagonal in shape and well-aligned. The diameters of some hexagonal ZnO nanorods were measured to be between 133.8 and 146.9 nm. The influence of bath temperature on hydrothermal development of ZnO_2 nanorods was investigated. According to the FESEM results, the average nanorod length and diameter increase linearly, indicating highly anisotropic growth. The nanorods manufactured at 80°C had the highest PCE (3.62%) (Kannan et al., 2020). Straight up aligned zinc oxide (ZnO) nanorods were electrochemically deposited on FTO substrate seeded with ZnO. The solutions were

synthesized with varying percentages of hexamethylenetetramine (HMTA). The efficiency of DSSCs based on ZnO photoanodes deposited from 0.0mM and 9.0mM HMTA solutions was 1.79 and 3.75%, respectively; this indicates an influence of HMTA on efficiency (Marimuthu et al., 2018). The FE-SEM analysis of synthesized samples by microwave-assisted and hydrothermal methods reveals the agglomerated environment of spherical particles and ZnO NRs. This rod-like structure could be attributed to preferential growth along the (0001) direction. The finding reveals the least, average, and greatest lengths of the ZnO NRs, which are 241.49, 646.73, and 941.16nm, respectively (Senthilkumar et al., 2018)

7. Review of Experimental Results and Discussion

ZnO nanorods have become more focused in nanoscience research, especially vertically aligned ZnO nanorods. It has been learned that the ability to control the size and morphology of nanorods is dependent on how the seed layer is manipulated.

7.1 Effect of temperature on seed layer morphology

Figure 2 depicts a SEM image of a 10 nm thick ZnO seed layer. The particles are spherical and uniform in size, density, and compactness. The particles were uniformly distributed, indicating that nucleation occurred in a homogeneous manner during seed layer deposition all over the substrate.

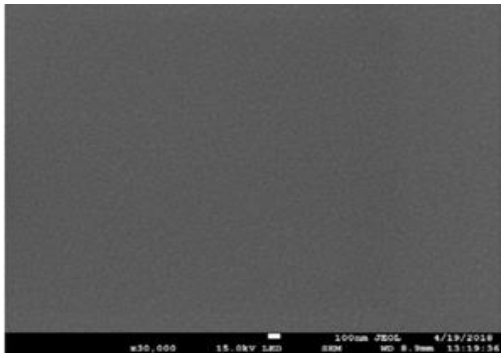

Figure 2. Top-view SEM image of ZnO seed layer deposited by ultrasonic spray pyrolysis Reproduced from (Mosalagae et al., 2020) with permission, copyright@2020, Elsevier

Figure 3 represents the morphology dependence of nanorods with temperature. Evidence from SEM results reveals that the length of nanorods increased from 400 nm to 700 nm as the temperature increased, and the average diameter of the grown nanorods increased from 129 nm to 143 nm. However, increasing the temperature reduces the compactness of the rods, which may be due to a rapid reaction growth rate at 90^0C.

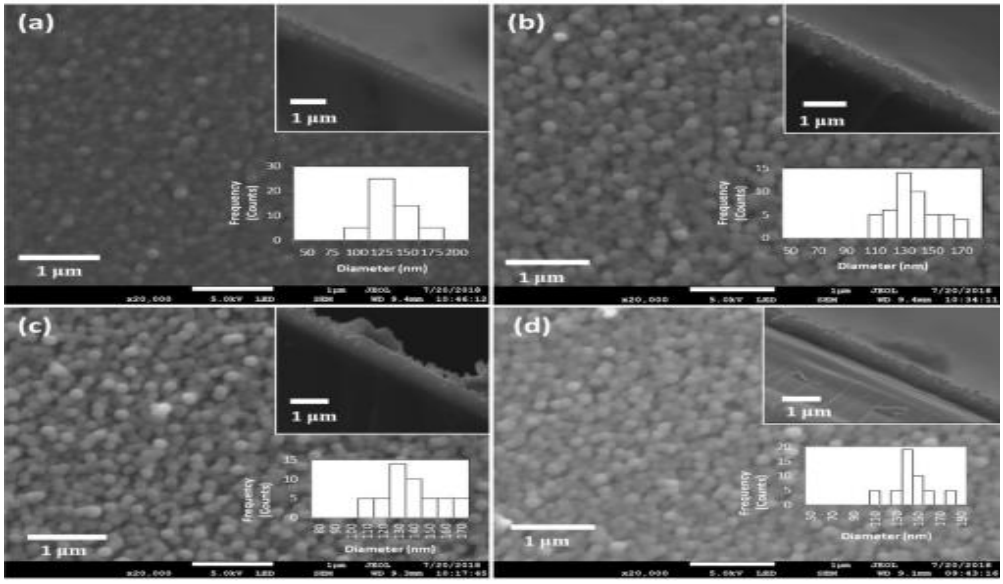

Figure 3. Top-view and cross-sectional view (insert) SEM images of ZnO nanorods grown at (a) 60^0C; (b) 70^0C; (c) 80^0C; (d) 90^0C. Histogram inserts in each SEM image represent nanorods diameter distribution. Reproduced from (Mosalagae et al., 2020) with permission, copyright@2020, Elsevier

Figure 4 shows FESEM images of ZnO seed layers heat treated at various temperatures. The images of fig 4 (a) and (b) reveal that raising the annealing temperature from 200^0C to 300^0C has no effect on the average size of particles of the ZnO seed layer (from 25.5mm to 26mm). The grain size of ZnO seed annealed at 400^0C is reduced from 26 nm to 14.4 nm in Fig. 4(c). At this annealing temperature, a recrystallization step takes place. As a result, this is one of the most favorable seeds for the emergence of ZnO nanorods via hydrothermal reaction. Figure 4 (d) shows that increasing the temperature to 500^0C causes the grain size to rise to 31.3nm. At this point, the atoms consolidate into the modified ones, resulting in grain coarseness.

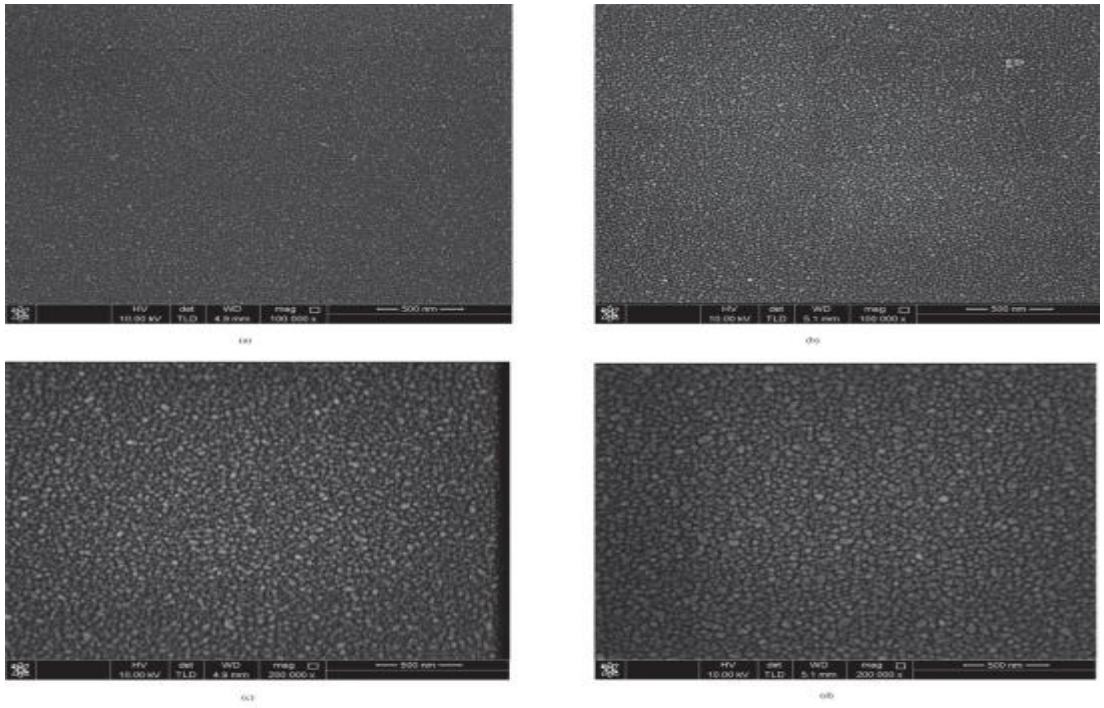

FIGURE 4. Surface morphologies of ZnO seeds annealed at different temperatures; (a) 200^0C, (b) 300^0C, (c) 400^0C, and (d) 500^0C, Reproduced from (Azzez et al., 2016) with permission, copyright@2015, AIP Publishing

Fig 5 presents the relation between the concentration of the solution and the size of the nanorods. When the concentrations of $Zn(NO_3)_2$ and methenamine was increased from 0.05 to 0.1M; the average diameter of the good facet hexagonal ZnO nanorods increased from 55nm to 170nm, and the length increased from1m to 1.3m. The length and diameter are proportional to the concentration of the solution, the size of the seed, and the time frame of growth.

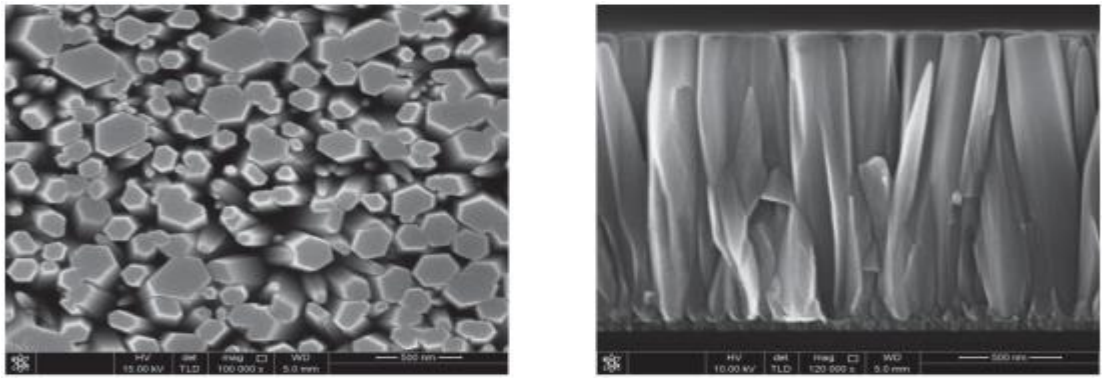

Figure 5. FESEM image of ZnO nanorods grown at 0.1M precursor concentration (a) Plan view (b) Cross section of view Reproduced from (Azzez et al., 2016) with permission, copyright@2015, AIP Publishing

7.2 Effect of seed layer thickness on the morphology of ZnO NRs

Figure 6: FE-SEM images of ZnO NRs grown on various thicknesses of the ZnO seed layer. As shown, enhancing the thickness of the ZnO seed layer from 10 nm to 40 nm had a significant effect on the length, diameter, and orientation of ZnO NRs. At 10, 20, 30, and 40nm, the grain size of the ZnO seed layer is 9.76, 11.57, 14.69, and 14.86nm, respectively. Thus, the thickness of 40 nm is the greatest in this test set. According to the images, increasing the thickness of the ZnO seed layer increased the average diameter of the ZnO NRs from 50.77nm to $85.67\ \text{nm}$. The study established the relationship between ZnO NRs and the particle size of the ZnO seed.

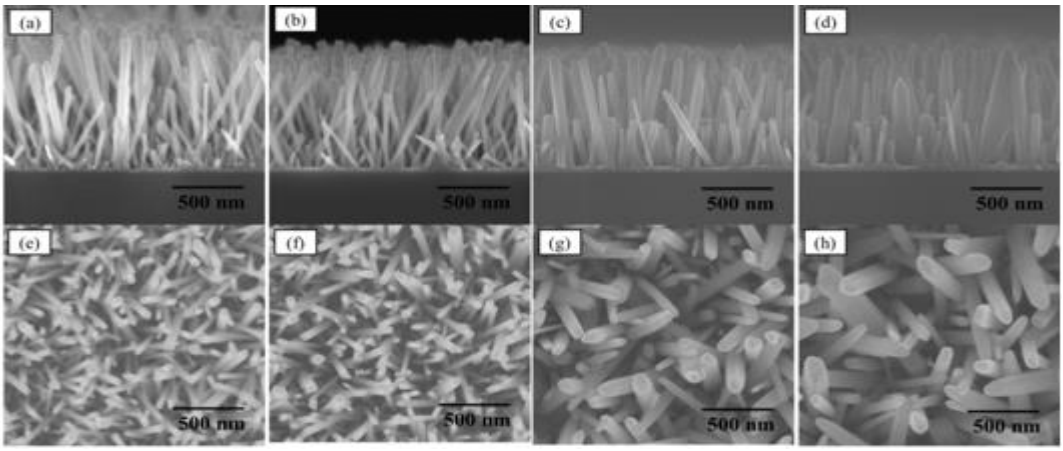

Fig. 6. FE-SEM images of ZnO NRs grown on different ZnO seed layer thicknesses which (a, e) 10 nm; (b, f) 20 nm; (c, g) 30 nm; (d, h) 40 nm. Reproduced from (Pokai et al., 2017) with permission, copyright@2017, Elsevier

7.3 Effect of precursor solution on seed layer morphology

A clear zinc acetate solution, a ZnO colloidal solution, and powdered ZnO spread in ethanol were used to make preparations for three different seed layers for the synthesis of ZnO nanorods. The scanning electron microscopy image indicates that the colloidal coating solution covers the deposited seed layer better than the solution or powder coating solutions. The cross-sectional SEM images show that the colloidal coating solution almost completely covers the FTO surface with the ZnO seed layer, whereas the powder coating solution only partially covers the FTO surface. Regardless of coating solutions, the deposited seed layers have been viewed to be composed of ZnO nanoparticles

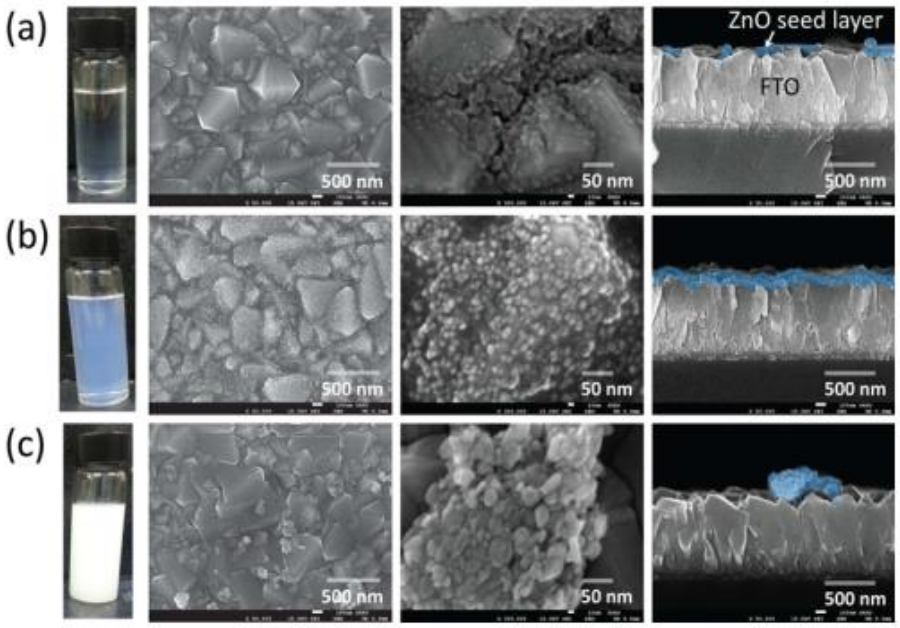

Fig. 7 SEM (surface and cross-sectional) images of the seed layers for growth of ZnO nanorods formed by (a) a clear solution, (b) a colloidal solution, and (c) dispersed powder solution. Reproduced from (Son et al., 2015) with permission, Copyright@American Chemical Society.

Cross-sectional SEM images of ZnO NRs grown on formed seed layers are shown in Figure 8. On the seed layers formed by the zinc acetate and colloidal coating solutions, ZnO NRs with a diameter of about $60\ \mathrm{nm}$ and a length of about $600\ \mathrm{nm}$ is observed; meanwhile, the seed layer deposited by the powder coating solution has a bigger diameter of about $120\ \mathrm{nm}$. The clustered ZnO nanoparticles in the seed layer are responsible for the larger diameter.

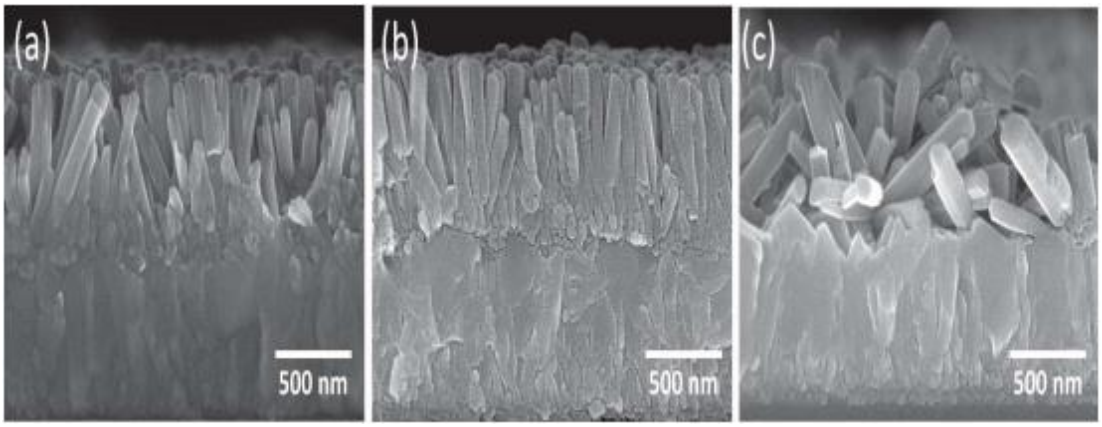

Fig. 8 SEM (Cross-sectional) images of ZnO nanorods grown on the seed layers prepared by (a) solution, (b) colloidal, and (c) powder precursor solutions. Reproduced from (Son et al., 2015) with permission, Copyright@American Chemical Society

7.4 Effect of higher sputtering power and working pressure on seed layer morphology

Fig 1 shows a FESEM image of a thin film formed by varying the sputtering working pressure (argon) and sputter power from $1.5X10^{-3}\ to\ 1.0X10^{-2}\mathrm{mbar}$ and from 50 to 200 W, respectively. Sample codes TF1, TF2, TF3, and TF4 were used to represent the seed layer image under the stated conditions, and all samples had a good size distribution. For TF1, TF2, TF3, and TF4, the grain sizes are 16.2, 18.9, 16.8, and $16.5\ \mathrm{nm}$, respectively. This is due to variation of the peak intensity ratio of the highest plane (002) to the second highest plane (100)

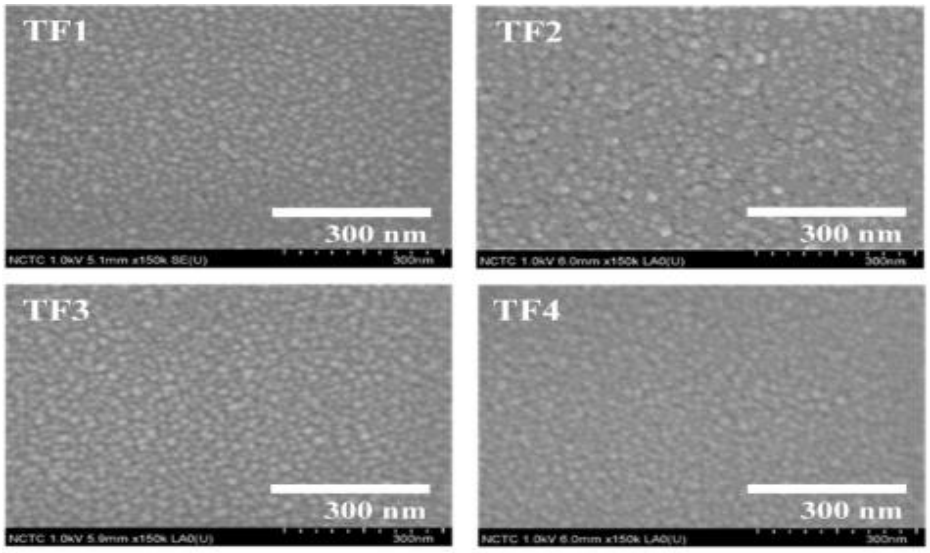

Figure 9. SEM images of ZnO seed layers. Reproduced from (Thongma et al., 2018) with permission, copyright@2018, Elsevier

Figure 2 shows SEM (Cross-sectional) pictures of ZnO nanorods developed on those seed layers. For TF1, TF2, TF3, and TF4, the peak intensity ratios (200) / (100) are 178, 563, 1076, and 2287, respectively. The results revealed that the (002) / (100) ratio has a significant impact on ZnO nanorod alignment. The greater the ratio, the greater the fraction of the nanorods aligned.

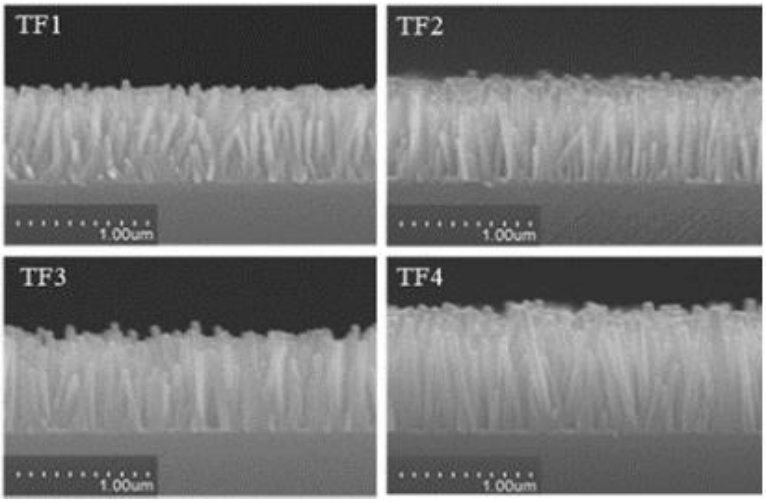

Fig. 10. a) SEM (Cross-sectional) images of ZnO nanorods grown on seed layers. Reproduced from (Thongma et al., 2018) with permission, copyright@2018, Elsevier

8. Conclusion

A photoanode's components of DSSC include a metal oxide semiconductor. Zinc oxide is an example of a metal oxide having a wide bandgap that functions as both electron carriers and dye adsorption surfaces. A lot of work is being done to achieve controlled morphology of ZnO NRs base photoanodes so that they can be used more effectively in DSSC applications because of their unique properties. Although there are many ways for synthesizing ZnO NRs, the work studied the factors that influence morphology. According to the available literature, controlling the seed layer thickness, solution concentration, and annealing thin film can improve NRs formation.

Funding: This research received no external funding.

Conflicts of Interest: The authors declare no conflict of interest.

Publisher's Note: All claims expressed in this article are solely those of the authors and do not necessarily represent those of their affiliated organizations, or those of the publisher, the editors and the reviewers.

References

[1] Azzez, S. A., Hassan, Z., Hassan, J. J., Alimanesh, M., Rasheed, H. S., Sabah, F. A., & Abdulateef, S. A. (2016). Hydrothermal synthesis of highly crystalline ZnO nanorod arrays: Dependence of morphology and alignment on growth conditions. *AIP Conference Proceedings*, *1733*. https://doi.org/10.1063/1.4948852

[2] Baruah, S., & Dutta, J. (2009). Hydrothermal growth of ZnO nanostructures. *Science and Technology of Advanced Materials*, *10*(1). https://doi.org/10.1088/1468-6996/10/1/013001

[3] Bera, S., Sengupta, D., Roy, S., & Mukherjee, K. (2021). Research into dye-sensitized solar cells: A review highlighting progress in India. *JPhys Energy*, *3*(3). https://doi.org/10.1088/2515-7655/abff6c

[4] Boukhoubza, I., Khenfouch, M., Leontie, L., Achehboune, M., Doroftei, C., Carlescu, A., Bulai, G., Mothudi, B. M., Zorkani, I., & Jorio, A. (2021). Enhancement of the structural and morphological properties of ZnO/rGO nanocomposites synthesized by hydrothermal method. *Materials Today: Proceedings*, *53*(XXXX), 324–331. https://doi.org/10.1016/j.matpr.2021.04.634

[5] Bourfaa, F., Boutelala, A., Aida, M. S., Attaf, N., & Ocak, Y. S. (2020). Influence of Seed Layer Surface Position on Morphology and Photocatalysis Efficiency of ZnO Nanorods and Nanoflowers. *Journal of Nanomaterials*, *2020*. https://doi.org/10.1155/2020/4072351

[6] Carella, A., Borbone, F., & Centore, R. (2018). Research progress on photosensitizers for DSSC. *Frontiers in Chemistry*, *6*(SEP), 1–24. https://doi.org/10.3389/fchem.2018.00481

[7] Chalangar, E., Nur, O., Willander, M., Gustafsson, A., & Pettersson, H. (2021). Synthesis of Vertically Aligned ZnO Nanorods Using Sol-gel Seeding and Colloidal Lithography Patterning. *Nanoscale Research Letters*, *16*(1). https://doi.org/10.1186/s11671-021-03500-7

[8] Edalati, K., Shakiba, A., Vahdati-Khaki, J., & Zebarjad, S. M. (2016). Low-temperature hydrothermal synthesis of ZnO nanorods: Effects of zinc salt concentration, various solvents, and alkaline mineralizers. *Materials Research Bulletin*, *74*, 374–379. https://doi.org/10.1016/j.materresbull.2015.11.001

[9] Faisal, A. D., Ismail, R. A., Khalef, W. K., & Salim, E. T. (2020). Synthesis of ZnO nanorods on a silicon substrate via hydrothermal route for optoelectronic applications. *Optical and Quantum Electronics*, *52*(4), 1–12. https://doi.org/10.1007/s11082-020-02329-1

[10] Fang, L., Li, H., Ma, X., Song, Q., & Chen, R. (2020). Optical properties of ultrathin ZnO films fabricated by atomic layer deposition. *Applied Surface Science*, *527*(May), 146818. https://doi.org/10.1016/j.apsusc.2020.146818

[11] Jacak, J. E., & Jacak, W. A. (2022). Routes for Metallization of Perovskite Solar Cells. *Materials*, *15*(6). https://doi.org/10.3390/ma15062254

[12] Kannan, S., Subiramaniyam, N. P., & Lavanisadevi, S. U. (2020). Controllable synthesis of ZnO nanorods at different temperatures for

enhancement of dye-sensitized solar cell performance. *Materials Letters*, *274*, 127994. https://doi.org/10.1016/j.matlet.2020.127994

[13] Kouhestanian, E., Ranjbar, M., Mozaffari, S. A., & Salaramoli, H. (2021). Investigating the Effects of Thickness on the Performance of ZnO-Based DSSC. *Progress in Color, Colorants and Coatings*, *14*(2), 101–112.

[14] Kumar, V., Gupta, R., & Bansal, A. (2021). Hydrothermal Growth of ZnO Nanorods for Use in Dye-Sensitized Solar Cells. *ACS Applied Nano Materials*, *4*(6), 6212–6222. https://doi.org/10.1021/acsanm.1c01012

[15] Lee, J. H., & Park, B. O. (2003). Transparent conducting ZnO: Al, In, and Sn thin films deposited by the sol-gel method. *Thin Solid Films*, *426*(1–2), 94–99. https://doi.org/10.1016/S0040-6090(03)00014-2

[16] Marimuthu, T., Anandhan, N., & Thangamuthu, R. (2018). Electrochemical synthesis of one-dimensional ZnO nanostructures on ZnO seed layer for DSSC applications. *Applied Surface Science*, *428*, 385–394. https://doi.org/10.1016/j.apsusc.2017.09.116

[17] Mbuyisa, P. N., Ndwandwe, O. M., & Cepek, C. (2015). Controlled growth of zinc oxide nanorods synthesized by the hydrothermal method. *Thin Solid Films*, *578*, 7–10. https://doi.org/10.1016/j.tsf.2015.02.002

[18] Mosalagae, K., Murape, D. M., & Lepodise, L. M. (2020). Effects of growth conditions on properties of CBD synthesized ZnO nanorods grown on ultrasonic spray pyrolysis deposited ZnO seed layers. *Heliyon*, *6*(7), e04458. https://doi.org/10.1016/j.heliyon.2020.e04458

[19] Nowak, E., Szybowicz, M., Stachowiak, A., Koczorowski, W., Schulz, D., Paprocki, K., Fabisiak, K., & Los, S. (2020). A comprehensive study of structural and optical properties of ZnO bulk crystals and polycrystalline films grown by sol-gel method. *RSC Advances*, *10*(7), 42838–42859. https://doi.org/10.1007/s00339-020-03711-2

[20] Pallikkara, A., & Ramakrishnan, K. (2020). Efficient charge collection of photoanodes and light absorption of photosensitizers: A review. *International Journal of Energy Research*, *45*(2), 1–24. https://doi.org/10.1002/er.5941

[21] Parisi, A., Pernice, R., Andò, A., Cino, A. C., Franzitta, V., & Busacca, A. C. (2017). Electro-optical characterization of ruthenium-based dye-sensitized solar cells: A study of light soaking, ageing and temperature effects. *Optik*, *135*, 227–237. https://doi.org/10.1016/j.ijleo.2017.01.100

[22] Pavithra, N., Asiri, A. M., & Anandan, S. (2015). Fabrication of dye-sensitized solar cell using gel polymer electrolytes consisting of poly(ethylene oxide)-acetamide composite. *Journal of Power Sources*, *286*(January), 346–353. https://doi.org/10.1016/j.jpowsour.2015.03.160

[23] Pokai, S., Limnonthakul, P., Horprathum, M., Eiamchai, P., Pattantsetakul, V., Limwichean, S., Nuntawong, N., Porntheeraphat, S., & Chitichotpanya, C. (2017). Influence of seed layer thickness on well-aligned ZnO nanorods via hydrothermal method. *Materials Today: Proceedings*, *4*(5), 6336–6341. https://doi.org/10.1016/j.matpr.2017.06.136

[24] Resmini, A., Tredici, I. G., Cantalini, C., Giancaterini, L., De Angelis, F., Rondanina, E., Patrini, M., Bajoni, D., & Anselmi-Tamburini, U. (2015). A simple all-solution approach to the synthesis of large ZnO nanorod networks. *Journal of Materials Chemistry A*, *3*(8), 4568–4577. https://doi.org/10.1039/c4ta05207b

[25] Rho, W. Y., Jeon, H., Kim, H. S., Chung, W. J., Suh, J. S., & Jun, B. H. (2015). Recent progress in dye-sensitized solar cells for improving efficiency: TiO2 nanotube arrays in the active layer. *Journal of Nanomaterials*, *2015*. https://doi.org/10.1155/2015/247689

[26] Safriani, L., Nurrida, A., Mulyana, C., Susilawati, T., Bahtiar, A., & Aprilia, A. (2017). Calculation of DSSC parameters based on ZnO nanorod/TiO2 mesoporous photoanode. *IOP Conference Series: Earth and Environmental Science*, *75*(1). https://doi.org/10.1088/1755-1315/75/1/012004

[27] Savari, R., Rouhi, J., Fakhar, O., Kakooei, S., Pourzadeh, D., Jahanbakhsh, O., & Shojaei, S. (2021). Development of photo-anodes based on strontium-doped zinc oxide-reduced graphene oxide nanocomposites for improving the performance of dye-sensitized solar cells. *Ceramics International*, *47*(22), 31927–31939. https://doi.org/10.1016/j.ceramint.2021.08.079

[28] Senthilkumar, N., Vivek, E., Shankar, M., Meena, M., Vimalan, M., & Potheher, I. V. (2018). Synthesis of ZnO nanorods by one-step microwave-assisted hydrothermal route for electronic device applications. *Journal of Materials Science: Materials in Electronics*, *29*(4), 2927–2938. https://doi.org/10.1007/s10854-017-8223-5

[29] Shakeel Ahmad, M., Pandey, A. K., & Abd Rahim, N. (2017). Advancements in the development of TiO2 photoanodes and its fabrication methods for dye-sensitized solar cell (DSSC) applications. A review. *Renewable and Sustainable Energy Reviews*, *77*(March), 89–108. https://doi.org/10.1016/j.rser.2017.03.129

[30] Siregar, N., Motlan, & Panggabean, J. (2020). The effect of magnesium (Mg) on structural and optical properties of ZnO: Mg thin film by sol-gel spin coating method. *Journal of Physics: Conference Series*, *1428*(1). https://doi.org/10.1088/1742-6596/1428/1/012026

[31] Son, D. Y., Bae, K. H., Kim, H. S., & Park, N. G. (2015). Effects of the seed layer on growth of ZnO nanorod and performance of perovskite solar cell. *Journal of Physical Chemistry C*, *119*(19), 10321–10328. https://doi.org/10.1021/acs.jpcc.5b03276

[32] Thongma, S., Boonkoom, T., Tantisantisom, K., & Krisdanurak, N. (2018). Influence of ZnO seed layer on the alignment of hydrothermal growth ZnO NR array and influence of surface area of metal contact on p-n junction diode behavior. *Materials Today: Proceedings*, *5*(7), 15203–15207. https://doi.org/10.1016/j.matpr.2018.04.083

[33] Verma, R., Gangwar, J., & Srivastava, A. K. (2017). Multiphase TiO2 nanostructures: A review of efficient synthesis, growth mechanism, probing capabilities, and applications in bio-safety and health. *RSC Advances*, *7*(70), 44199–44224. https://doi.org/10.1039/c7ra06925a

[34] Weerasinghe, H. C., Huang, F., & Cheng, Y. B. (2013). Fabrication of flexible dye-sensitized solar cells on plastic substrates. *Nano Energy*, *2*(2), 174–189. https://doi.org/10.1016/j.nanoen.2012.10.004

[35] Wibowo, A., Marsudi, M. A., Amal, M. I., Ananda, M. B., Stephanie, R., Ardy, H., & Diguna, L. J. (2020). ZnO nanostructured materials for emerging solar cell applications. *RSC Advances*, *10*(70), 42838–42859. https://doi.org/10.1039/d0ra07689a

[36] Yin, Y. T., Que, W. X., & Kam, C. H. (2010). ZnO nanorods on ZnO seed layer derived by sol-gel process. *Journal of Sol-Gel Science and Technology*, *53*(3), 605–612. https://doi.org/10.1007/s10971-009-2138-4

[37] Yoshimura, M., & Byrappa, K. (2008). Hydrothermal processing of materials: Past, present, and future. *Journal of Materials Science*, *43*(7), 2085–2103. https://doi.org/10.1007/s10853-007-1853-x